Predicting Typhoon Morakot's Catastrophic Rainfall with a Convection-Permitting Mesoscale Ensemble System

FUQING ZHANG AND YONGHUI WENG

Department of Meteorology, The Pennsylvania State University, University Park, Pennsylvania

YING-HWA KUO

National Center for Atmospheric Research, Boulder, Colorado

JEFFERY S. WHITAKER

NOAA/ESRL, Boulder, Colorado

BAOGUO XIE

Department of Atmospheric Sciences, Peking University, Beijing, China

(Manuscript received 26 February 2010, in final form 1 July 2010)

ABSTRACT

This study examines the prediction and predictability of the recent catastrophic rainfall and flooding event over Taiwan induced by Typhoon Morakot (2009) with a state-of-the-art numerical weather prediction model. A high-resolution convection-permitting mesoscale ensemble, initialized with analysis and flow-dependent perturbations obtained from a real-time global ensemble data assimilation system, is found to be able to predict this record-breaking rainfall event, producing probability forecasts potentially valuable to the emergency management decision makers and the general public. Since all the advanced modeling and data assimilation techniques used here are readily available for real-time operational implementation provided sufficient computing resources are made available, this study demonstrates the potential and need of using ensemble-based analysis and forecasting, along with enhanced computing, in predicting extreme weather events like Typhoon Morakot at operational centers.

1. Introduction

Floods associated with tropical cyclones are one of the most costly and deadly nature hazards in the world, particularly for the island of Taiwan, which possesses significant mesoscale topography (e.g., Wu et al. 2002; Cheung et al. 2008). From 6 to 10 August 2009, Typhoon Morakot brought record-breaking rainfalls and the worst flooding event over the island of Taiwan in 50 years, which claimed more than 600 lives with more than 200 people missing and an estimated $3.3 billion in damages. The worst-hit mountainous southern Taiwan recorded large areas of 72-h total precipitation close to 3000 mm (Fig. 1a). The maximum 24-h rainfall amounts were 1403 mm in 24 h at Weiliaoshan in Pingtung County on 8 August, and 2327 mm in 48 h at Alishan, Chiayi County on 8–9 August, both of which are new rainfall records and are not far from the world records of 1825 and 2467 mm, respectively.

The extreme rainfall amount was the consequence of moisture-laden typhoon circulation impinging upon the Central Mountain Range of Taiwan, with many peaks exceeding 3000 m. Typhoon Morakot was only a category 2 storm before it made landfall on Taiwan at around 1800 UTC 7 August 2009. However, the size of its circulation was fairly large in comparison to climatologically averaged values (Knaff et al. 2007) with gale-force wind extending to a 650-km radius. As a result, before Morakot's landfall on Taiwan, the northeasterly flow associated with the typhoon's outer circulation had already produced significant amounts of rainfall over southern Taiwan starting at 1200 UTC 6 August into 7 August 2009. Large amounts of rain continued to fall over

Corresponding author address: Dr. Fuqing Zhang, Dept. of Meteorology, The Pennsylvania State University, University Park, PA 16802. E-mail: fzhang@psu.edu

DOI: 10.1175/2010WAF2222414.1

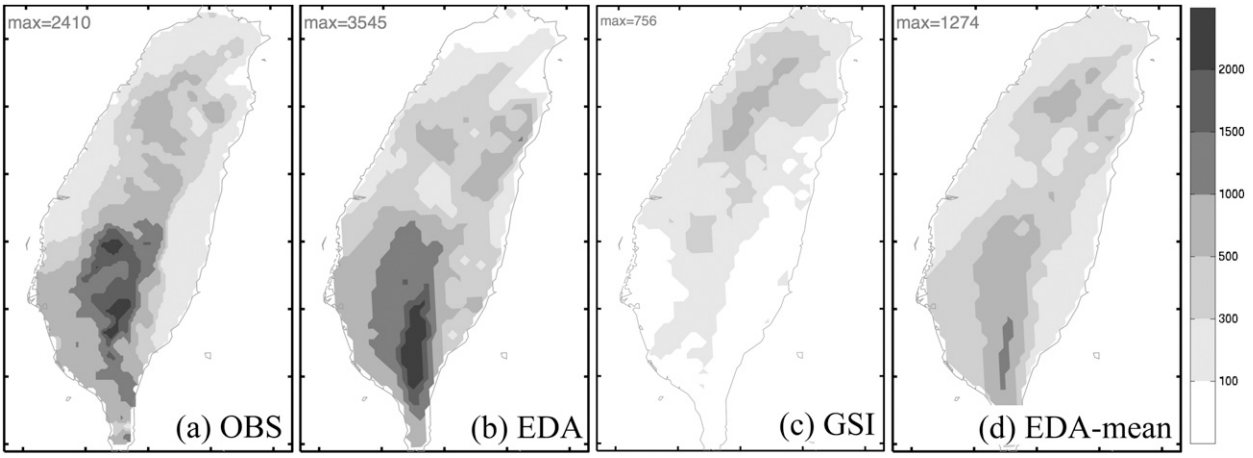

FIG. 1. The 72-h accumulated rainfall total (mm, from 0000 UTC 6 Aug to 0000 UTC 9 Aug) over Taiwan: (a) observational analysis provided by the CWB, (b) ARW 96-h forecast using the GFS real-time EDA analysis as the initial conditions (IC_EDA), (c) ARW 96-h forecast with the GFS operational analysis using GSI as the initial conditions (IC_GSI), and (d) ensemble mean of the 60-member ensemble forecast using the GFS real-time EDA perturbations as the initial conditions.

southern Taiwan from 1200 UTC 7 August into 8 August during the period when the storm made landfall and crossed over northern part of the island. After Morakot reemerged over the Taiwan Strait and moved northward, the southwesterly flow associated with the storm's outer circulation continued to produce very heavy rainfall over southern Taiwan. The continued heavy rainfall over southern Taiwan for three consecutive days, before, during, and after landfall, eventually triggered enormous mudslides and severe flooding throughout southern Taiwan.

The prediction of such a heavy rainfall event is exceedingly challenging for any dynamical operational model. Such a model must have sufficient resolution to resolve the mesoscale Central Mountain Range. Accurate representation of the complex interaction between the terrain and the slow-moving typhoon vortex is likely one of key factors in the rainfall forecasts. Moreover, in order to predict the storm's track accurately, the large-scale environment, particularly the moisture distribution, must be accurately analyzed. Third, to predict the intensity and structure of the storm, the typhoon vortex needs to be properly initialized. Finally, the hydrological cycles must be properly modeled or parameterized to accurately predict precipitation amounts and distributions. It is desirable to have a model at convection-permitting[1] resolution that permits the use of explicit cloud microphysics for precipitation prediction. For these reasons, accurate prediction of the torrential rainfall associated with typhoon–mountain interaction for a case such as Morakot will require the use of a high-resolution convection-permitting model with accurate synoptic-scale analyses and vortex initialization. However, because of uncertainties in large-scale analyses, vortex initialization, and physical parameterization, a single deterministic run is often subject to considerable errors and uncertainties. For the Morakot event, even if a single deterministic forecast predicted an extreme rainfall amount, the forecasters would be hesitant to take such a forecast at its face value, as the uncertainties for such a forecast can be substantial and could potentially lead to embarrassing false alarms. To help the forecaster predict a devastating event such as Morakot, we need to provide not only the forecast itself, but also the uncertainties of the forecast (probability prediction). This will require the use of an ensemble forecast system at convection-permitting resolution. This study seeks to explore the predictability[2] of this record-breaking rainfall event with the state-of-the-art science and technology that is readily available but

[1] It is generally understood that the so-called convection-permitting simulations may capture the basic nonhydrostatic dynamics of a convective cell, but not the smaller-scale turbulence mixing associated with individual cumulus cloud; the convective-resolving experiments would require a grid scale well within the inertial subrange of moist cumulus convection (see, e.g., Bryan et al. 2003).

[2] There are different measures of predictability (Lorenz 1969, 1996; Zhang et al. 2002, 2003, 2006). *Intrinsic predictability* can be defined as "the extent to which prediction is possible if an optimum procedure is used" in the presence of infinitesimal initial errors (Lorenz 1969). *Practical predictability*, on the other hand, can be specified as the ability to predict based on the procedures that are currently available. Practical predictability is limited by realistic uncertainties in both the initial states and the forecast models, which in general are not infinitesimally small (Lorenz 1996). The later will be the focus of the current study.

has not yet been implemented at operational weather prediction centers.

2. Data and methodology

We perform a total of 62 convection-permitting simulations of the Morakot event with the Advanced Research version (ARW) of the next-generation mesoscale Weather Research and Forecast Model (WRF) currently being developed and employed at the National Center for Atmospheric Research (Skamarock et al. 2005). Two model domains coupled through two-way nesting are employed; the fine (coarse) domain has a horizontal grid spacing of 4.5 (13.5) km covering areas of 2700 × 2400 (8100 × 7200) km^2. The model has 35 vertical levels with physics configurations that are the same as those used in Zhang et al. (2009). These high-resolution convection-permitting ARW forecasts were initialized at 0000 UTC 5 August (~2.5 days before landfall): one initialized with the National Centers for Environmental Prediction (NCEP) operational analysis (global statistical interpolation or GSI) of the Global Forecast System (GFS) (IC_GSI), one with the analysis (ensemble mean) from an experimental real-time global Ensemble Data Assimilation (EDA) system (IC_EDA-DF), and the other 60 with ensemble perturbations (IC_EDA-EF, labeled from m11 to m70) that represent the flow-dependent analysis uncertainty of the global EDA system (hereafter referred to as the control ensemble). This real-time EDA system based on the ensemble Kalman filter (EnKF) technique (Whitaker et al. 2008) uses the same GFS model and assimilates the same set of observations as those in NCEP operational GSI analyses, and has demonstrated advantages over the current NCEP operational system owing to its use of a more advanced data assimilation technique (Hamill et al. 2011).

Both the experimental global EDA analysis and all the convection-permitting ARW simulations are performed at the ''Ranger'' Linux cluster of the Texas Advanced Computing Center (TACC) under the auspices of the Hurricane Forecast Improvement Project (HFIP). Each ARW simulation runs on 256 Ranger cluster cores with a wall-clock time of ~10 h for a 5-day integration. The TACC Ranger cluster is capable of carrying out all of these convection-permitting simulations simultaneously in real time.

The observational rainfall shown in Fig. 1a is plotted with the 0.02° × 0.02° gridded rainfall estimate provided by the Taiwan Central Weather Bureau and available hourly.

3. ARW ensemble forecast results

Figure 2 shows the tracks, intensities,[3] and sizes (15 m s^{-1} wind radii) of Typhoon Morakot from the two deterministic forecasts (IC_EDA-DF and IC_GSI) and the 60 ensemble members in comparison with the operational best-track analysis (observations) provided by the Japan Meteorological Agency (JMA). Despite a noticeable northward (southward) bias of Morakot's track in the ARW forecast of IC_EDA-DF in the early (later) part of the simulation, the simulated storm follows the observed storm reasonably well before, during, and after its landfall over Taiwan (Fig. 2a). The position forecast error by IC_EDA-DF at 1800 UTC 7 August near the time of landfall with a lead time of 66 h is only 47 km (Fig. 3), which is very small compared to the official track error at 2–3-day range according to the official National Oceanic and Atmospheric Administration/National Hurricane Center (NOAA/NHC) projections Franklin 2009). Figure 4 shows the 700-hPa geopotential height and wind forecasts from IC_EDA-DF (and the average of the five best-performing members; more on this subject later) at 0000 UTC 7 August (before landfall) and 0000 UTC 8 August (after landfall) that verify reasonably well against the GFS final (FNL) analysis in terms of both position and storm asymmetry. Both the IC_EDA-DF forecast and the FNL analysis have stronger mid- to low-level wind speed in the southeast quadrant than other quadrants and a dilation axis along the southwest–northeast direction. On the other hand, the FNL-analyzed inner-core vortex is significantly weaker than in the IC_EDA-DF forecast, which is likely due to the use of coarser resolution and/or the deficiency of the data assimilation method in the FNL analysis. The track and position forecasts by IC_EDA-DF are in stark contrast to the ARW forecasts initialized with the operational GFS analysis using the GSI method (IC_GSI). The simulated storm in the IC_GSI forecast dissipated before reaching Taiwan, and did not make landfall (not shown).

The intensity forecast as measured by the maximum surface winds from IC_EDA-DF is also remarkably good through the 4-day forecast period after the initial adjustment during the first day (Fig. 2b). The EDA analysis did not employ vortex bogussing or relocation, ad hoc techniques that are widely used in operational tropical cyclone prediction systems. In contrast, GSI uses

[3] The JMA best-track intensity estimate refers to a 10-min-average sustained wind speed for the western Pacific tropical cyclones while the 10-m maximum wind speed interpolated from the instantaneous ARW model output are used for all simulations in this study.

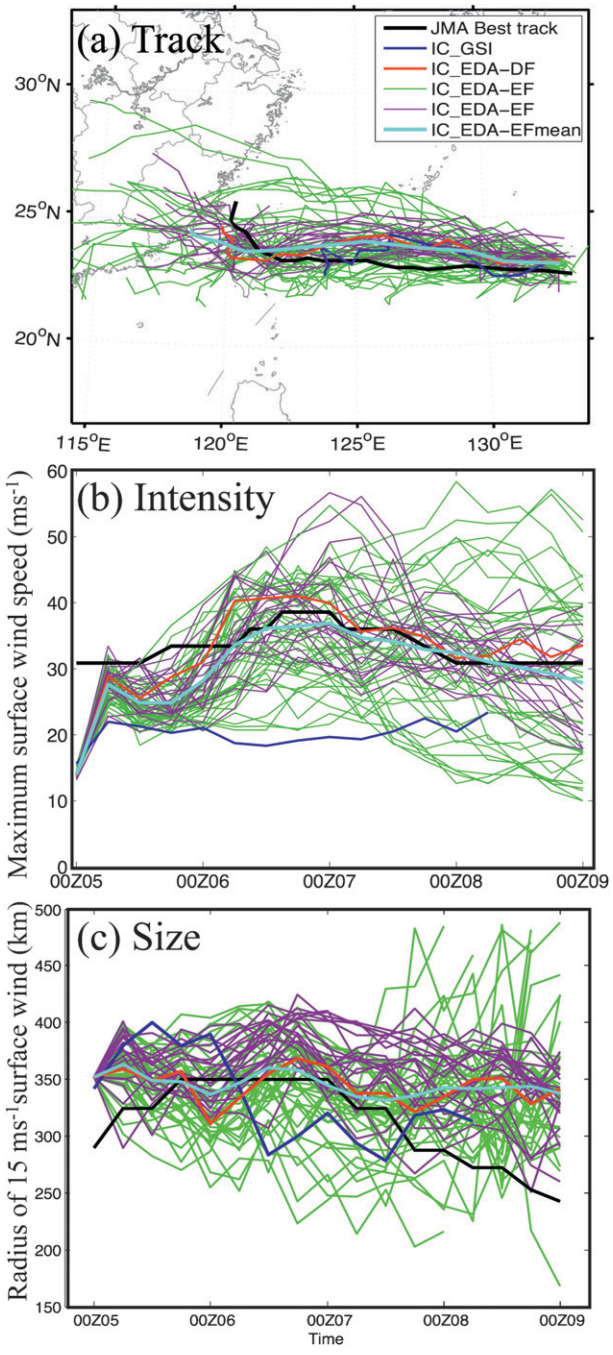

FIG. 2. (a) Track, (b) intensity (10-m maximum wind speed), and (c) size (15 m s^{-1} wind radius) forecasts of Morakot from 60 ARW ensemble members (green and purple), the ensemble mean (cyan), and ARW forecasts using EDA (red) and GSI (blue) analyses as initial conditions in comparison with the operational best-track analysis (black) of the JMA. Thin purple curves denote the 20 members that have the best rainfall forecasts shown in Fig. 6.

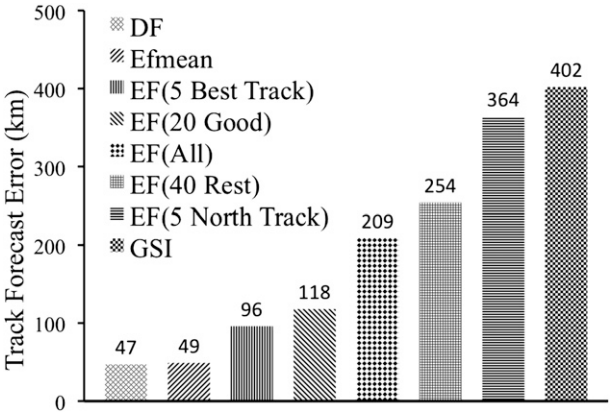

FIG. 3. The position errors of various forecasts (distance from the JMA best-track estimate) near the time of Morokot's landfall in Taiwan valid at 1800 UTC 7 Aug 2009: IC_EDA-EF(20Good) is the average track error of the 20 members that have good rainfall forecasts (m11, m13, m15, m16, m19, m22, m23, m26, m29, m31, m33, m37, m39, m46, m47, m49, m57, m61, m64, and m70), IC_EDA-EF(40Rest) is the average of the other 40 members, IC_EDA-EF(All) is the averaged position error of all ensemble members, IC_EDA-EF(5BestTrack) is the average track error of the five members (m11, m13, m19, m47, and m61) that have the best-track forecasts, IC_EDA-EF(5NorthTrack) is the average track error of the five members (m21, m27, m52, m54, and m55) that have the northern-most (poor) track forecasts during the time of landfall, and IC_EDA-EFmean is the position error of the ensemble mean track.

a vortex relocation scheme that first moves the GFS background vortex to the best-track location and then performs the standard GSI analysis (Q. Liu, NCEP, 2010, personal communications; information also available online at http://www.nws.noaa.gov/om/tpb/472.htm). The initial vortex in IC_GSI is substantially weaker than that of IC_EDA-DF, especially at lower levels (Figs. 5a–c). As a consequence, the IC_GSI produces a poor intensity forecast for Morakot (Fig. 2b).

In addition, the size of Morakot, measured by the maximum radius of 15 m s^{-1} surface winds, is also reasonably forecasted by IC_EDA-DF (Fig. 2c) except for the last day of the forecast period after the typhoon has crossed over Taiwan. Note that there are significant uncertainties in the current mostly satellite-based observational tropical-cyclone size estimates, including that by JMA, as shown here. Note also that after the typhoon made landfall, there are also significant uncertainties in estimating its track, size, and intensity from the model given strong variations near the surface due to high variations in the terrain. Nevertheless, the JMA size estimate in terms of 15 m s^{-1} surface wind radii is for the most part consistent with two other independent size estimates, one obtained through aircraft dropsondes (C.-C. Wu 2010, personal communications) and the other from

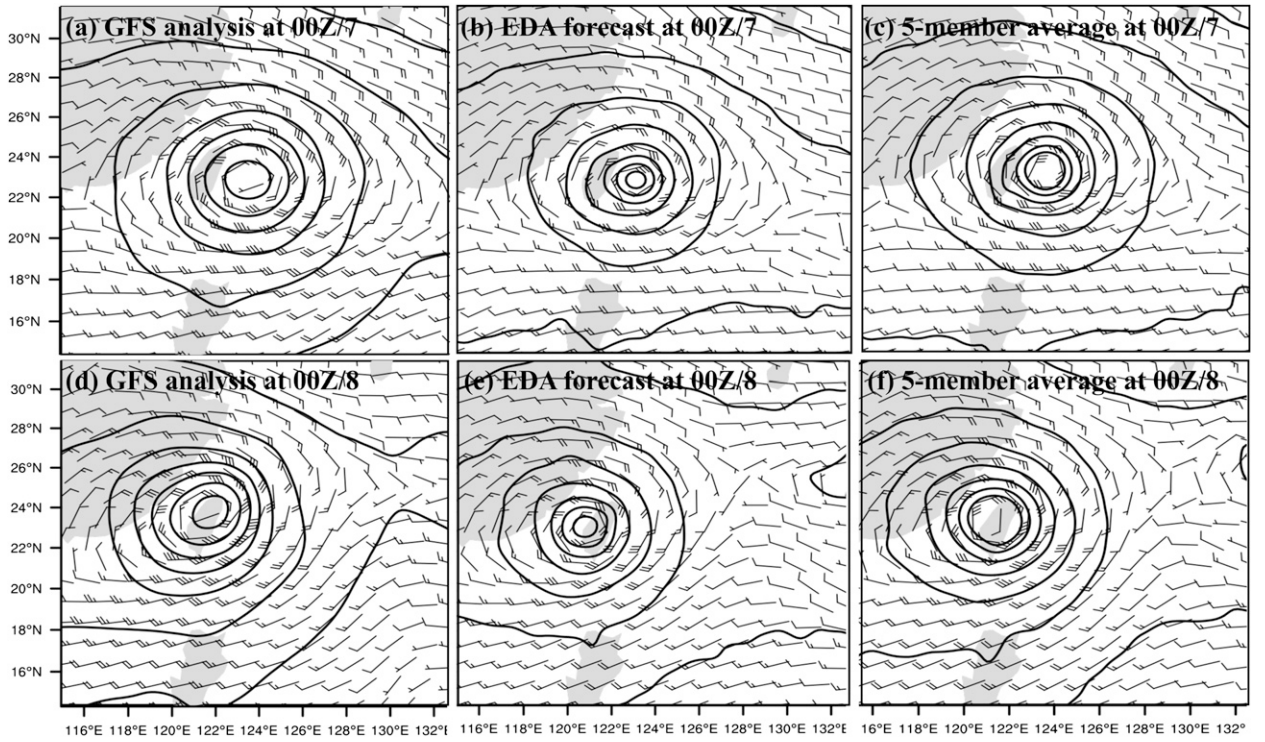

FIG. 4. Verification of the 700-hPa height (contoured every 40 m from 2860 to 3160 m) and wind forecasts by IC_EDA-DF and the mean of the five best-track members (m11, m13, m19, m47, and m61) against the GFS FNL analysis at (a)–(c) 0000 UTC 7 Aug and (d)–(f) 0000 UTC 8 Aug 2009 before and after Morakot's observed landfall in Taiwan.

Quick Scatterometer (QuikSCAT) satellite-derived surface winds (C.-S. Lee 2010, personal communications).

Among the track, intensity, and size forecasts made by the ARW control ensemble (IC_EDA-EF), we see a large disparity between the ensemble members, which indicates a large uncertainty in predicting the exact location, track, size, and intensity of Morakot 24–96 h in advance (Fig. 2). Nevertheless, most of ensemble members did make landfall within 12 h of the observed time. The mean position error averaged over all ensemble members near the time of Morakot's landfall in Taiwan with 66 h of lead time is 209 km (Fig. 3), which is below the average operational forecast error for Atlantic hurricanes from the National Hurricane Center (Franklin 2009). The track error of the ensemble mean position near the time of landfall is 49 km, similar to the deterministic forecast of IC_EDA-DF (47 km), both of which are greatly smaller that that of the position error averaged over all of the ensemble members (Fig. 3).

Consistent with the track and intensity forecasts, Figs. 1b–d show the 72-h accumulated rainfall over Taiwan ending at 0000 UTC 9 August with a 96-h forecast lead time predicted by experiment IC_EDA-DF and IC_GSI as well as by the ARW ensemble mean, respectively. Compared to the gridded observations in Fig. 1a, experiment IC_EDA-DF forecast initialized with the EDA analysis performed remarkably well on the record-breaking rainfall in terms of both location and intensity throughout the area of Taiwan. Most notably, compared to rainfall observations obtained from the Taiwan Central Weather Bureau (CWB; see Fig. 1a), the areas of total 72-h accumulated precipitation are forecasted accurately by IC_EDA-DF over southern Taiwan, where Morakot hit the hardest. Even the area coverage of the total 72-h accumulated precipitation exceeding 2000 mm is well forecasted, despite a substantial shift to the south and greater rainfall amounts in the model. The observed secondary precipitation maximum over north-central Taiwan is also reasonably well forecasted by the IC_EDA-DF experiment, though there is an apparent overprediction along the northeast coast of the island. This northern secondary precipitation maximum is also simulated by the IC_GSI experiment but IC_GSI almost completely misses the large areas of extreme rainfall over the southern part of the island (Fig. 1c).

Given the limited predictability of tropical cyclones due to moist convection (e.g., Zhang and Sippel 2009) and the deficiency/uncertainty in numerical weather prediction models including ARW, it is speculated that

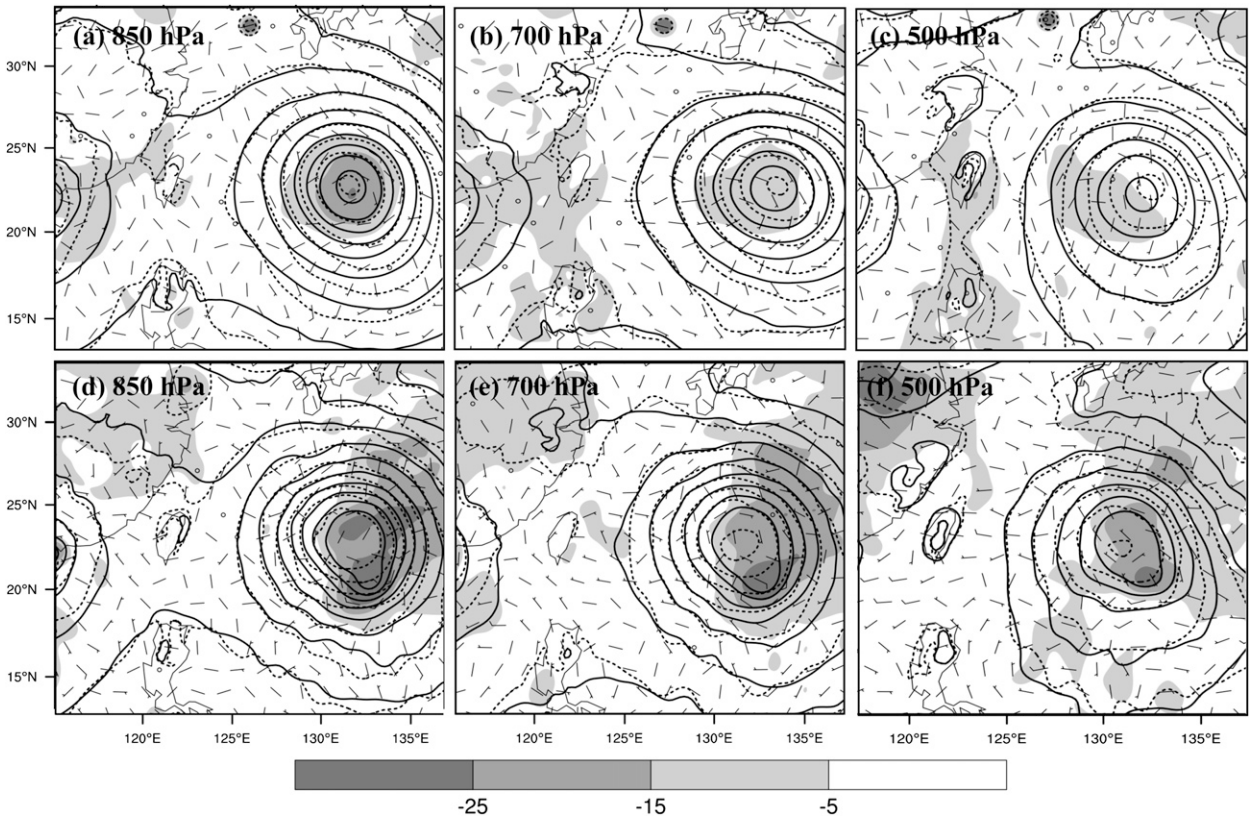

FIG. 5. (a)–(c) The differences in the initial condition winds (full barb, 10 m s^{-1}) and difference geopotential heights (shaded, m) between the EDA (dashed contours) and GSI (solid contours) analyses at (a) 850, (b) 700, and (c) 500 hPa. (d),(f) As in (a),(c), but for the differences between the five best-track members (dashed contours) and the five northern-most-track members (solid contours) at (d) 850, (e) 700, and (f) 500 hPa, respectively. The dashed and solid contours are the analysis geopotential heights (every 20 m).

even if a successful deterministic forecast such as IC_EDA-DF were available in real time, operational forecasters will have a difficult time assessing its validity given the unprecedented nature of this record-breaking flooding event. Having an ensemble forecast available in real time would allow forecasters to better assess the uncertainties of the forecasts (e.g., Toth and Kalnay 1993). Figure 6 shows the 72-h rainfall total over Taiwan using all 60 ensemble members that were initialized with flow-dependent analysis uncertainties from the EDA; the rainfall total averaged over all ensemble members is shown in Fig. 1d.

As in the track and intensity forecasts, indeed there is a large spread (and thus large uncertainties) in the 72-h precipitation total between the 60 ensemble members over the hardest-hit area in southern Taiwan. Two members (m21 and m27) completely failed to produce any significant precipitation (<100 mm total) over southern Taiwan and nine others combined for an accumulated total of less than 300 mm over the most severely flooded areas. On the other hand, there are more than 20 (10) members that forecasted a maximum 72-h total of over 1000 (2000) mm in the vicinity of the observed maximum location. The 20 members that have the best rainfall forecasts are highlighted with violet colors in Fig. 2, from which it is clear that, on average, the better the track position and intensity forecast, the better the rainfall forecasts. The averaged position error at 1800 UTC 7 August for these 20 members is 118 km, which is less than half of the average of the remaining 40 members (254 km, as shown in Fig. 3). Furthermore, the averaged position error of the five best-track forecast members (with the smallest root-mean-square error calculated every 6 h during the 0- and 96 h forecasts, i.e., m11, m13, m19, m47, and m61) is only 96 km while the average position error of the five members that have the northern-most track forecasts (m21, m27, m52, m54, and m55) is 364 km (Fig. 3) at 1800 UTC 7 August. The mean 700-hPa geopotential height and wind forecasts averaged over these five best-track forecast members before and after Morakot's landfall in Taiwan also verified well against the FNL analysis and the IC_EDA-EF forecasts in terms of position, size, and asymmetry (Fig. 4). The initial geopotential and wind differences between

FIG. 6. The 72-h accumulated rainfall total (mm, gray scale as in Fig. 1) over Taiwan, forecasted by each of the 60 ensemble members. The 20 members that have good rainfall forecasts (m11, m13, m15, m16, m19, m22, m23, m26, m29, m31, m33, m37, m39, m46, m47, m49, m57, m61, m64, and m70) are denoted by pink curves in Fig. 2, among which the five members m11, m13, m19, m47, and m61 have the best track forecasts. Members m21, m27, m52, m54, and m55 are the five that have the northern-most (poor) track forecasts during the time of landfall.

the mean of the five best-track forecast members and the mean of the five northern-most track (poor forecast) members at different levels are shown in Figs. 5d–f, which show that the best members tend to have a stronger cyclonic circulation to the southeast of the initial vortex. On average, these five best-track forecast members also have higher middle-level moisture close to the initial TC vortex (not shown).

However, there are a few members that have rather small position errors but fail to produce good rainfall forecasts (not shown), indicating only factors that are also affecting the rainfall predictability. On the other hand, the strong differences between the deterministic forecast of IC_EDA-DF and the mean of all of the ensembles in terms of both track and precipitation (Figs. 1 and 2) suggest there are strong nonlinearities associated with the evolution of Morakot, which further highlights the need for probabilistic forecasts.

Based on the ensemble forecasts, Fig. 7 shows the ensemble-generated probability distribution for the 72-h accumulated rainfall totals with different thresholds. Consistent with individual member forecasts in Fig. 6, it is

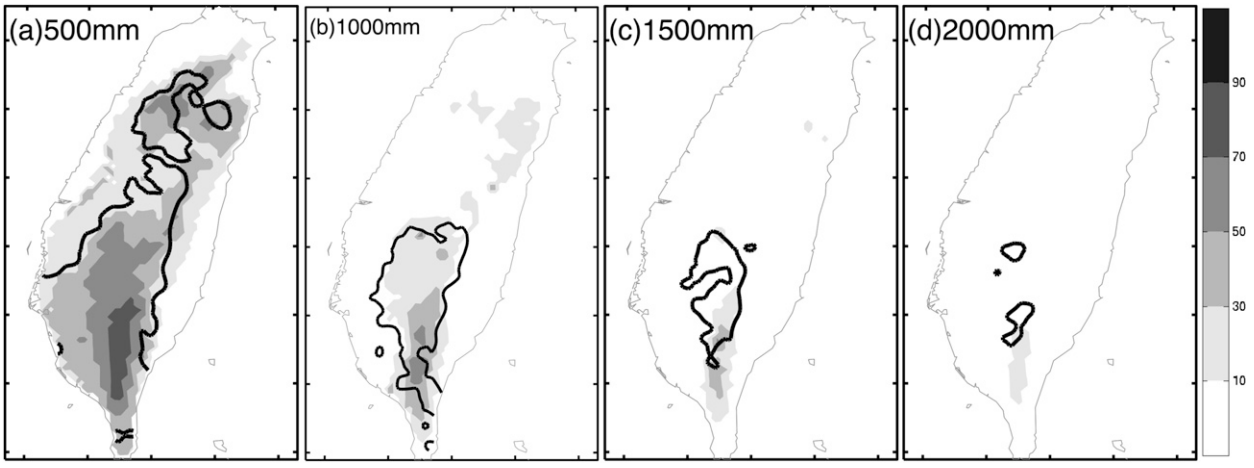

FIG. 7. Probability distribution (%) of the potential rainfall exceeding threshold values of (a) 500, (b) 1000, (c) 1500, and (d) 2000 mm estimated from the 60-member ARW ensemble initialized with EDA perturbations. The same threshold value of the observed rainfall in each panel is denoted with solid contours.

shown that the probability of the total 72-h accumulated precipitation exceeding 500 mm is over 70% in the hardest-hit flooding area, and over 30% throughout southern Taiwan and some parts of north-central Taiwan (most of these areas have observed rainfalls exceeding 500 mm as in Fig. 1a). The probability of the 72-h total rainfall exceeding 1000 (1500) mm is over 50% (30%) in the heaviest-flooding area. Moreover, as rare as it was, the probability of the total precipitation exceeding 2000 mm is higher than 10% in a small area over southern Taiwan that is not far from the area with the most observed rainfall. All of these probability forecasts, along with the deterministic run of IC_EDA-DF, could have been very valuable to the forecasters if they were made available in real time. For example, such probability forecasts, even at the 10–30% level, can be used by emergency management officers employing simple cost–benefit analyses in decision-making systems to decide on whether to make additional preparations or to evacuate people from the potential disaster areas 3–4 days in advance.

Three additional ensemble experiments are performed in the same manner as the control 4.5-km ARW ensemble but with only 30 members and with different initial conditions (only the means of these sensitivity ensembles are shown in Fig. 8). An ensemble initialized

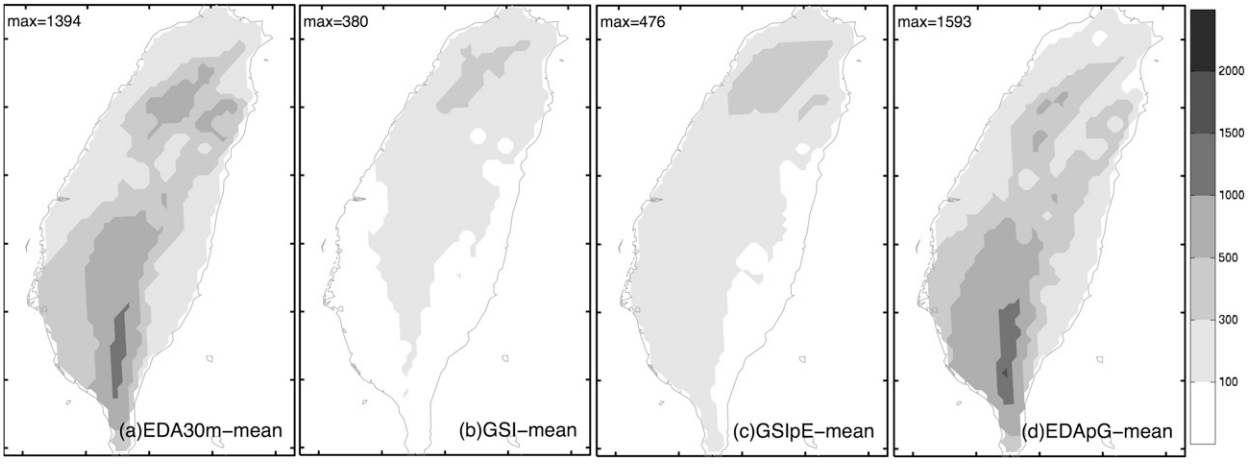

FIG. 8. Ensemble mean forecast of the 72-h accumulated rainfall total (mm; from 0000 UTC 6 Aug to 0000 UTC 9 Aug) over Taiwan from (a) ''EDA30m,'' a subset of IC_EDA consisting of 30 randomly selected members in IC_EDA; (b) a 30-member ensemble that is initialized by adding climatological uncertainties derived from the ARW 3DVAR default background error covariance as perturbations to the GSI analysis; (c) a 30-member ensemble that is initialized by adding the same EDA perturbations as in EDA30m to the GSI analysis; and (d) a 30-member ensemble that is initialized by adding the same 3DVAR perturbations as in ensemble GSI to the EDA mean analysis.

by adding climatological uncertainties derived from the ARW three-dimensional variational data assimilation (3DVAR) default background error covariance as perturbations (Barker 2005) to the GSI analysis fails to capture the record-breaking event in southern Taiwan entirely (Fig. 8b). The second ensemble initialized by adding 30 randomly selected EDA perturbations from the control ensemble (IC_EDA) to the GSI analysis performs slightly better, with nearly a third of the members predicting a maximum of over 500 mm in accumulated rainfalls but no member has rainfall exceeding 1000 mm over the flooding area (Fig. 8c). A third ensemble initialized by adding the same 3DVAR perturbations to the EDA mean analysis performs similarly to the control ensemble in terms of its ensemble mean but the ensemble spread is too small to reflect realistic uncertainties for this event, with both the track and intensity nearly completely biased on one side of the observations (Fig. 8d). These additional sensitivity ensemble experiments further highlight the significance of using flow-dependent initial condition uncertainties in the ensemble forecast, consistent with the findings from tropical cyclone predictions with global-model ensembles (Hamill et al. 2011). These experiments also highlight the importance of creating an accurate large-scale analysis (e.g., through EDA) as the basis for a cloud-permitting ensemble system.

In other words, for the Morakot case, we needed to have a good synoptic-scale analysis and associated uncertainty, which are provided by the global EDA. We then needed a good high-resolution cloud-permitting model with appropriate physics and detailed topography. Moreover, as demonstrated in Zhang et al. (2009) and Torn and Hakim (2009), additional improvements may be expected if the EDA analysis is further performed with a cloud-permitting regional-scale ensemble analysis and forecast system, especially through the inclusion of inner-core observations such as those from Doppler radars and/or aircraft dropsondes.

4. Concluding remarks

In this study, we have experimented with a GFS-based ensemble data assimilation system, which is followed by ensemble prediction using a high-resolution (4.5 km) WRF model with explicit microphysics. We showed that the global EDA system produced the initial analysis that leads to a much more successful deterministic 4-day prediction of the heavy rainfall over southern Taiwan. The WRF forecast initialized with the operational GSI analysis failed to predict a significant storm, and significant rainfall over Taiwan. This case demonstrates that a global EDA system may provide significant improvements over the current 3DVAR-based GSI system.

Convection-permitting mesoscale ensemble forecasts, initialized with flow-dependent perturbations from global EnKF analyses, were able to predict this extreme, record-breaking flooding event, producing probability forecasts that are potentially valuable to the emergency management decision makers and the general public. All the advanced modeling and data assimilation techniques used in this study are readily available for real-time operational implementation, provided sufficient computing resources are made available.

Acknowledgments. This work was supported in part by the NOAA Hurricane Forecast Improvement Project (HFIP), Office of Naval Research Grants N000140410471 and N000140910526, and National Science Foundation Grant ATM-0840651. The computing for this study was performed at the Texas Advanced Computing Center. Thanks are due to Bob Gall and Fred Toepfer for suggesting the color-coding scheme used in Fig. 2.

REFERENCES

Barker, D. M., 2005: Southern high-latitude ensemble data assimilation in the Antarctic Mesoscale Prediction System. *Mon. Wea. Rev.,* **133,** 3431–3449.

Bryan, G. H., J. C. Wyngaard, and J. M. Fritsch, 2003: Resolution requirements for the simulation of deep moist convection. *Mon. Wea. Rev.,* **131,** 2394–2416.

Cheung, K. K. W., L.-R. Huang, and C.-S. Lee, 2008: Characteristics of rainfall during tropical cyclone periods in Taiwan. *Nat. Hazards Earth Syst. Sci.,* **8,** 1463–1474.

Franklin, J. L., cited 2009: The 2008 National Hurricane Center verification report. [Available on line at http://www.nhc.noaa.gov/verification/pdfs/Verification_2008.pdf.]

Hamill, T. M., J. S. Whitaker, M. Fiorino, and S. G. Benjamin, 2011: Global ensemble predictions of 2009's tropical cyclones initialized with an ensemble Kalman filter. *Mon. Wea. Rev.,* in press.

Knaff, J. A., and Coauthors, 2007: Statistical tropical cyclone wind radii prediction using climatology and persistence. *Wea. Forecasting,* **22,** 781–791.

Lorenz, E. N., 1969: The predictability of a flow which possesses many scales of motion. *Tellus,* **21,** 289–307.

——, 1996: Predictability—A problem partly solved. *Proc. Seminar on Predictability,* Vol. I, Reading, United Kingdom, ECMWF, 1–19.

Skamarock, W. C., J. B. Klemp, J. Dudhia, D. O. Gill, D. M. Barker, W. Wang, and J. G. Powers, 2005: A description of the Advanced Research WRF version 2. NCAR Tech. Note 468+STR, 88 pp.

Torn, R. D., and G. J. Hakim, 2009: Ensemble data assimilation applied to RAINEX observations of Hurricane Katrina (2005). *Mon. Wea. Rev.,* **137,** 2817–2829.

Toth, Z., and E. Kalnay, 1993: Ensemble forecasting at NMC: The generation of perturbations. *Bull. Amer. Meteor. Soc.,* **74,** 2317–2330.

Whitaker, J. S., T. M. Hamill, X. Wei, Y. Song, and Z. Toth, 2008: Ensemble data assimilation with the NCEP Global Forecast System. *Mon. Wea. Rev.,* **136,** 463–482.

Wu, C.-C., T.-H. Yen, Y.-H. Kuo, and W. Wang, 2002: Rainfall simulation associated with Typhoon Herb (1996) near Taiwan. Part I: The topographic effect. *Wea. Forecasting,* **17,** 1001–1015.

Zhang, F., and J. A. Sippel, 2009: Effects of moist convection on hurricane predictability. *J. Atmos. Sci.,* **66,** 1944–1961.

——, C. Snyder, and R. Rotunno, 2002: Mesoscale predictability of the ''surprise'' snowstorm of 24–25 January 2000. *Mon. Wea. Rev.,* **130,** 1617–1632.

——, ——, and ——, 2003: Effects of moist convection on mesoscale predictability. *J. Atmos. Sci.,* **60,** 1173–1185.

——, A. Odins, and J. W. Nielsen-Gammon, 2006: Mesoscale predictability of an extreme warm-season rainfall event. *Wea. Forecasting,* **21,** 149–166.

——, Y. Weng, J. A. Sippel, Z. Meng, and C. H. Bishop, 2009: Cloud-resolving hurricane initialization and prediction through assimilation of Doppler radar observations with an ensemble Kalman filter. *Mon. Wea. Rev.,* **137,** 2105–2125.